Stratiform precipitation, vertical heating profiles, and the Madden-Julian Oscillation

Jialin Lin[1,2], Brian Mapes[1], Minghua Zhang[2] and Matthew Newman[1]

[1] **NOAA-CIRES Climate Diagnostics Center, Boulder, Colorado**
[2] **State University of New York, Stony Brook, New York**

November, 2002

Submitted to *Journal of the Atmospheric Sciences*

ABSTRACT

The contribution of stratiform precipitation to the vertical profile of heating in the Madden-Julian Oscillation (MJO) is examined. Heating profiles in a strong MJO event in 1992-3 are calculated from the Tropical Ocean Global Atmosphere (TOGA) Coupled Ocean Atmosphere Response Experiment (COARE) sounding array data. Long-term heating estimates, derived from vorticity budgets in NCEP reanalysis, support the notion that this well-observed event was representative. Convective/stratiform precipitation estimates are obtained from the Tropical Rainfall Measurement Mission (TRMM) satellite. All datasets are filtered using a 30-70 day bandpass filter. The long-term MJO composites are constructed using linear correlation and linear regression with respect to time series of surface precipitation.

The observed MJO anomalous vertical heating profile is very top-heavy at the time of maximum precipitation. TRMM data show that the anomalous stratiform precipitation contributes more than 50% to the anomalous total precipitation in the MJO. This large fraction of stratiform precipitation significantly increases the anomalous heating in the upper troposphere and decreases the anomalous heating in the lower troposphere. This helps to make the heating profile top-heavy.

The MJO anomalous vertical heating profiles in several GCMs and other models are shown to differ from the observations. The model heating profiles are generally middle-heavy.

Based on the above results, it is hypothesed that the weak and fast MJO in the current GCMs may be partly caused by their *middle-heavy anomalous vertical heating*

profiles.

1. Introduction

Discovered by Madden and Julian (1971, 1972), the Madden-Julian Oscillation (MJO) is the dominant intraseasonal mode in tropical convection and circulation (e.g. Weickmann et al. 1985, Lau and Chan 1985, Salby and Hendon 1994, Wheeler and Kiladis 1998). It affects a wide range of tropical weather such as the onset and breaks of the Indian and Australian summer monsoons (e.g. Yasunari 1979, Hendon and Liebmann 1990), and the formation of tropical cyclones (e.g. Nakazawa 1986, Liebmann et al. 1994). It also drives teleconnections to the extratropics (e.g., Lau and Phillips 1986, Winkler et al. 2001) and impacts some important extratropical weather. On a longer timescale, the MJO is observed to trigger or terminate some El Nino events (e.g. Kessler et al. 1995, Takayabu et al. 1999, Bergman et al. 2001). Therefore, the MJO is important for both extended-range weather forecasting and long-term climate prediction.

Fig. 1a shows the standard deviation of the 30-70 day bandpass filtered anomaly of CPC Merged Analysis of precipitation (CMAP, see section 2 and 3 for details of the data and filtering). This intraseasonal variability has two heating centers, one in the Indian ocean, the other in the western Pacific. Fig. 1b shows the lag-correlation between the 30-70 day CMAP precipitation anomaly at 0N155E and the same quantity everywhere along the equator. The propagating part of intraseasonal variability (hereafter called the MJO) moves eastward from the Indian Ocean to the western Pacific. The phase speed in these two heating centers is about 5 m/s (or 4 degrees/day).

The motivation of this study is that eastward-propagating signals in general circulation models (GCMs) are generally too weak and propagate too fast compared with observations (e.g. Hayashi and Sumi 1986, Hayashi and Golder 1986, 1988, Lau et al. 1988, Slingo et al. 1996). This shortcoming is detrimental to both numerical weather prediction and climate prediction. Theoretical studies may offer useful guidance on how to improve MJO simulations by GCMs, in particular how to make tropical variations stronger and propagate slower.

Observations suggest that the MJO in the eastern hemisphere is maintained by diabatic heating (Krishnamurti et al. 1985, Murakami and Nakazawa 1985, Yanai et al. 2000). The heating is strongly associated with a propagating large-scale circulation anomaly (e.g. Madden and Julian 1972, Weickmann et al. 1985, Salby and Hendon 1994), and this propagating circulation anomaly (hereafter called a "wave") also feeds back onto the heating (Hendon and Salby 1994, Zhang 1996), suggesting a wave-heating feedback theoretical framework for the MJO. In this view, the diabatic heating forces a certain kind of wave or large-scale circulation. This kind of large-scale circulation in turn influences the diabatic heating (somehow) in such a way that the whole disturbance may amplify, propagate, and decay. The heating may be divided into five components, namely the latent heatings associated with free troposphere moisture convergence, boundary layer moisture convergence, surface heat flux (latent plus sensible), and local moisture storage, as well as radiative heating. These five components have been emphasized in different types of theories historically, including the wave-CISK (Convective Instability of the Second Kind) mechanism (e.g.

Hayashi 1970, Lindzen 1974, Lau and Peng 1987, Zhang and Geller 1994), the frictional wave-CISK mechanism (e.g. Hayashi 1971, Wang and Rui 1990, Salby et al. 1994), the WISHE (Wave Induced Surface Heat Exchange) mechanism (e.g. Emanuel 1987, Neelin et al. 1987), the charge-discharge mechanism (e.g. Blade and Hartmann 1993, Wang and Schlesinger 1999), and the cloud-radiation interaction mechanism (Hu and Randall 1994, Raymond 2001, Lee et al. 2001), respectively.

Because diabatic heating plays a key role in the MJO, this study examines observed heating, and compares heating profiles in observations and models. The purpose is to look for possible ways to improve model simulations of the MJO.

The seasonal mean vertical heating profile over the tropical oceans has been derived from heat budget analysis of sounding arrays in several field experiments including Mashall Island (Yanai et al. 1973), GATE (e.g. Thompson et al. 1979), AMEX (e.g. Frank and McBride 1989), and TOGA COARE (Lin and Johnson 1996, Frank et al. 1996, Yanai et al. 2000, and Zhang and Lin 1999). The anomalous vertical heating profile for the MJO, which is the perturbation around the seasonal mean profile, has not been published, to our knowledge.

Stratiform precipitation is important to the vertical heating profile, because it is associated with heating in the upper troposphere and cooling in the lower troposphere, and thus shifts the heating peak upward (Houze 1982, 1989, 1997, Johnson 1984, Mapes and Houze 1995). The contribution of stratiform precipitation to the seasonal mean precipitation has been studied by many authors, but the contribution of anomalous stratiform precipitation to the anomalous precipitation in the MJO has not been reported, to our knowledge. In this study, we get this value from the Tropical Rainfall Measuring Mission (TRMM) satellite data.

The datasets used in this study are described in section 2. The methods are described in section 3. The results are reported in section 4. A summary is given in section 5.

2. Data

The datasets used include TOGA COARE data and long-term data.

The TOGA COARE datasets include:

(1) 120 day (November 1, 1992 to Feburary 28, 1993) of the 6-hourly diabatic heating profiles for the Intensive Flux Array (IFA, Fig. 1) calculated by Ciesilski et al. (2002).

(2) 120 day (November 1, 1992 to Feburary 28, 1993) of the daily diabatic heating profiles for the Outer Sounding Array (OSA, Fig. 1) calculated by Zhang and Lin (1999) using the method of Zhang and Lin (1997).

(3) 120 day (November 1, 1992 to Feburary 28, 1993) of the hourly radiative heating profiles for the IFA calculated by Qian and Cess (2002).

The long term datasets include:

(1) 21 years (1979-1999) of the pentad "chi-corrected" diabatic heating profiles calculated by Winkler et al. (2001). The horizontal resolution is 2.5 degree longitude by 2.5 degree latitude. We average the data along the equator (between 5N and 5S) with a zonal resolution of 10 degree longitude. The diabatic heating profiles are determined from an improved iterative solution of the "chi problem" (Sardesmukh

1993). This iterative procedure is applied to twice-daily NCEP reanalysis wind fields to minimize the nonlinear vorticity budget imbalance at 28 atmospheric levels, and the modified divergent wind circulation is further constrained to satisfy the large-scale mass budget. Diabatic heating rates are finally determined as a balance requirement in the heat budget, using the modified wind circulation to compute the other terms. See Sardesmukh (1993) for details of the technique.

(2) 21 years (1979-1999) of the pentad CMAP precipitation calculated by Xie and Arkin (1997). The horizontal resolution is 2.5 degree longitude by 2.5 degree latitude. We average the data along the equator (between 5N and 5S) with a zonal resolution of 5 degree longitude.

(3) 4 years (1998-2001) of the half-hourly TRMM gridded convective/stratiform precipitation (product number 3G68) calculated by Kummerow et al. (2000) and Stocker et al. (2001). The dataset contains convective/stratiform precipitation values from three algorithms: precipitation radar (PR), TRMM Microwave Imager (TMI), and combined algorithm. The horizontal resolution is 0.5 degree longitude by 0.5 degree latitude. We average the data along the equator (between 5N and 5S) to pentad data with a zonal resolution of 5 degree longitude.

3. Method

The MJO is a broadband phenomena with an averaged period of 45 days and a wide spread from 20 to 80 days (see review by Madden and Julian 1994). To emphasize the broadband nature of the oscillation, previous studies used wide frequency bands such as 30-60 days (Weickmann et al. 1985), 30-96 days (Wheeler and Kiladis 1998), or 10-95 days (Bantzer and Wallace 1996). In this study we also use a wide frequency band of 30-70 days. All datasets are filtered using a 30-70 day Murakami (1976) filter, whose response function is shown in Fig. 2. The central frequency correspond to a period of 45 days. The half amplitude is at periods of 30 days and 70 days. We have also tested the Lanczos filter (Duchan 1979), and the results are not sensitive to the different choice of filters.

For the TOGA COARE data, there are two MJO events (Fig. 3). We focus on the December 1992 event. This is a strong MJO event with its amplitude at the TOGA COARE location larger than two standard deviation of the 21 year data (Fig. 1a). It moves eastward with a phase speed of 5 m/s, which is similar to the phase speed of the 21 year composite (Fig. 1b). The maximum of the 30-70 day bandpass filtered precipitation anomaly at the TOGA COARE location occurs on December 20, 1992.

For the long term data, an MJO composite is constructed using linear regression with respect to an MJO index. In this study, we use filtered CMAP precipitation as our MJO index. Because the MJO is a large-scale phenomena dominated by wavenumber 0-6 (Wheeler and Kiladis 1998), the CMAP precipitation has been zonally filtered to keep only wavenumber 0-6. The confidence level of linear correlation is estimated following Oort and Yienger (1996).

4. Results

4.1 Observed vertical heating profile in the MJO

Fig. 4 shows the vertical structure of the diabatic heating anomaly in the MJO for (a) TOGA COARE IFA, (b) TOGA COARE OSA, and (c) 21 years (1979-1999) of chi-corrected data at 0N155E. In (c) only the anomaly with linear correlation above the 95% confidence level is plotted. The time lag is with respect to the time of maximum precipitation. The time evolution is from the right to the left, showing the local evolution of heating as the eastward-moving MJO passes the measurement longitude (Fig. 3, Fig. 1b). We can see that the heating has a slight westward phase tilt with height. It develops first in the lower troposphere and then shifts upward as it intensifies. This westward phase tilt with height may be associated with more shallow convection in the earlier stage, and more stratiform precipitation in the later stage.

Fig. 5 shows the vertical heating profile at the time of maximum precipitation for the above three different datasets. The three heating profiles look quite similar with each other. They are very top-heavy, i.e., with strong heating in the upper troposphere and weak heating in the lower troposphere.

What makes the anomalous heating profile in the MJO so top-heavy? From the work of Houze (1982, 1989, 1997) and Johnson (1984), we know that the stratiform precipitation associated with organized deep convective systems is characterized by heating in the upper troposphere associated with the mesoscale updraft, and cooling in the lower troposphere associated with the mesoscale downdraft. This has the effect of shifting the altitude of the heating peak of deep convective cloud systems upward. Therefore, next we look at how much the stratiform precipitation contributes to the anomalous precipitation in the MJO.

4.2 Contribution of stratiform precipitation to the heating profile

Fig. 6 shows the precipitation anomaly during the composite life cycle of the MJO for 4 years (1998-2001) of TRMM precipitation radar(PR), Microwave Imager (TMI), and combined data at 0N147E. The thick solid line is total precipitation, the thin solid line is convective precipitation, and the thin dashed line is stratiform precipitation. All the three datasets consistently show that the stratiform precipitation contributes more than 50% of the anomalous total precipitation. The climatological mean fraction of stratiform precipitation for the three datasets are 52%, 32%, and 47%, respectively. Although the values differ among the different datasets, the three datasets consistently show that the fraction of anomalous stratiform precipitation in the MJO is much larger than the climatological mean fraction of stratiform precipitation. Since the MJO is associated with more organized convective systems, such as the super cloud clusters (SCCs), the 2-day waves, and the mesoscale convective systems (e.g. Nakazawa 1988, Mapes and Houze 1993, Chen et al. 1996), it is possible that these organized convective systems are responsible for the large fraction of stratiform precipitation.

How much does this stratiform precipitation affect the vertical heating profile? Following the method of Johnson (1984), we partition the observed heating profile into three components: stratiform, radiative and convective (Fig. 7). The stratiform heating is assumed to have the profile observed in Johnson (1984). The 30-70 day anomalous radiative profile at the time of maximum precipitation is calculated from the hourly IFA radiative heating profiles by Qian and Cess (2002). The convective profile is derived as the residual from the total. The decomposition in Fig. 7 assumes the fraction of stratiform precipitation to be 0.3, which is the lower bound of the observed values with the consideration that some of the stratiform rainfall is condensed in the convective region and then transported to the stratiform region (Leary and Houze 1980, Gamache and Houze 1983, Johnson 1984). We can see that the stratiform precipitation significantly increases the heating in the upper troposphere and decreases the heating in the lower troposphere, which helps to make the heating profile top-heavy.

4.3 Comparison with the model heating profiles

Now we compare the observed MJO heating profile with several model MJO heating profiles (Fig. 8a). The models include the GFDL GCM (Lau et al. 1988), the University of Illinois GCM (Wang and Schlesinger 1999), the Seoul National University GCM (Lee et al. 2001), and one theorectical model (Sui and Lau 1989). The model MJO heating profiles are generally middle-heavy. For clarity, we plot the difference between the observed profile and the model profiles in Fig. 8b. The observed heating profile has stronger heating in the upper troposphere and weaker heating in the lower troposphere. This is similar to the stratiform heating profile, suggesting that the models may lack some equivalent of the observed anomalous stratiform precipitation.

The above results lead us to the following hypothesis: the weak and fast MJO in the current GCMs may be partly caused by their *middle-heavy anomalous vertical heating profiles.*

This hypothesis can be tested in the GCMs by adding some equivalent of the observed stratiform precipitation to make the diabatic heating profile top-heavy. There are two possible ways to do this. The first is to revise the convection schemes to include the mesoscale effects (with the observed magnitude). Some convection schemes (e.g. Molinari and Corsetti 1985, Sud and Walker 1993) have included the effect of mesoscale downdraft, and some schemes (e.g. Donner 1993, Alexander and Cotton 1998, Gray 2000, Donner et al. 2001) have included the effects of both mesoscale updraft and mesoscale downdraft. Donner et al. (2001) apply the Donner (1993) convection scheme in the GFDL GCM. The simulated seasonal mean fraction of stratiform precipitation agrees well with the TRMM observation. The MJO simulation is reported to be improved (Donner 2002, presentation in the Seventh Annual CCSM Workshop), but further diagnostics need to be done to determine whether the model MJO heating profile becomes more top-heavy. The second way of adding equivalent of stratiform precipitation is to encourage more precipitation to occur via the large-scale (resolved) condensation and microphysics schemes, by assuming some fraction of the convective condensate falls through air with large-scale mean humidity (e.g. Randall et al. 1989, Tiedtke 1993, Fowler and Randall 1996, Del Genio et al. 1996, Li et al. 2002). This modification has been shown to be important for improving the mean state simulation, but its effect on the MJO simulation has not been published.

Some cautions need to be taken when applying the above modifications to a GCM: (1) These modifications may change the mean state of the GCM, which may also affect the amplitude and phase speed of the model MJO. We need to seperate the effect of heating profile from that of the mean state. (2) These modifications may induce the response of some other schemes, such as the shallow convection scheme, which may cancel the intended change in the final diabatic heating profile. Therefore we need to plot the final diabatic heating profile to see if it is really top-heavy.

This hypothesis can also be examined in theoretical models of the effect of vertical heating profiles on wave-heating feedbacks. Within the context of wave-CISK theory (Yamasaki 1968a, 1968b, 1969, Chang and Lim 1988, Sui and Lau 1989, Cho and Pendlebury 1997), the heating profile is specified outright, allowing direct study of the influence of profile shape. Cho and Pendlebury (1997) decomposed the specified heating profile into vertical modes, and found that instability required a sufficient amplitude of the full-wave mode, with heating above cooling, corresponding directly to the stratiform contribution to heating profiles. Yamasaki (1968a, 1968b, 1969) suggested in his numerical modeling studies that some tropical systems are unstable only if the cumulus heating profile has a maximum in the upper troposphere. Sui and Lau (1989) found that a "deep convection" heating profile (lighter dash-dot line in Fig. 8) increases the propagation speed of disturbances, compared to the case with a shallower heating profile. At first glance, this suggests that more top-heavy heating will make faster, not slower, waves, but in fact their "deep convection" heating profile is middle-heavy with strong heating in the lower troposphere, although its mathematical maximum is in the upper troposphere. Therefore their comparison was between bottom-heavy and middle-heavy heating profiles. It might more generally be true that theories which attatch importance to higher vertical modes - whether by top-heavy or bottom-heavy excitation - will tend to generate slower-propagating modes. All of the above studies parameterize the heating using the free troposphere moisture convergence, so their conclusions apply only to the wave-CISK mode. It is also interesting to examine the effect of vertical heating profile on the wave-heating feedback when including the boundary layer moisture convergence (emphasized by the frictional wave-CISK mechanism), the surface heat flux (emphasized by the WISHE mechanism), and the local moisture storage (emphasized by the charge-discharge mechanism).

5. Summary

Diabatic heating profiles calculated from the Tropical Ocean Global Atmosphere (TOGA) Coupled Ocean Atmosphere Response Experiment (COARE) sounding array and the long-term NCEP reanalysis, supplemented by the convective/stratiform precipitation from TOGA COARE and Tropical Rainfall Measurement Mission (TRMM) satellite, are used to study the contribution of the stratiform precipitation to the vertical heating profile in the MJO. All datasets are filtered using a 30-70 day bandpass filter. The long-term MJO composites are constructed using linear correlation and linear regression with respect to precipitation.

The observed MJO anomalous vertical heating profile is very top-heavy at the time of maximum precipitation. TRMM data show that the anomalous stratiform precipitation contributes more than 50% to the anomalous total precipitation in the MJO. This large fraction of stratiform precipitation significantly increases the anomalous heating in the upper troposphere and decrease the anomalous heating in the lower troposphere. This helps to make the heating profile top-heavy.

The MJO anomalous vertical heating profiles in several current GCMs and other models are shown to differ from the observations. The model heating profiles are generally middle-heavy.

Based on the above results, we have the following hypothesis: the weak and fast MJO in the current GCMs maybe partly caused by their middle-heavy anomalous vertical heating profiles.

REFERENCES

Alexander, G. D., and W. R. Cotton, 1998: The use of cloud-resolving simulations of mesoscale convective systems to build a mesoscale parameterization scheme. *J. Atmos. Sci.*, **55**, 2137-2161.

Bantzer, C. H., and J. M. Wallace, 1996: Intraseasonal variability in tropical mean temperature and precipitation and their relation to the tropical 40-50 day oscillation. *J. Atmos. Sci.*, **53**, 3032-3045.

Bergman, J. W., H. H. Hendon, K. M. Weickmann, 2001: Intraseasonal Air-Sea Interactions at the Onset of El Nino. *J. Climate*, **14**, 1702-1719.

Blade, I., and D. L. Hartmann, 1993: Tropical intraseasonal oscillations in a simple nonlinear model. *J. Atmos. Sci.*, **50**, 2922-2939.

Chang, C. P., and H. Lim, 1988: Kelvin wave-CISK: A possible mechanism for the 30-50 day oscillations. *J. Atmos. Sci.*, **45**, 1709-1720.

Chen, S. S., R. A. Houze., and B. E. Mapes, 1996: Multiscale variability of deep convection in relation to large-scale circulation in TOGA COARE. *J. Atmos. Sci.* , **53**, 1380-1409.

Cho, Han-Ru, D. Pendlebury, 1997: Wave CISK of Equatorial Waves and the Vertical Distribution of Cumulus Heating. *J. Atmos. Sci.*, **54**, 2429-2440.

Ciesilski, P. E., R. H. Johnson, and J. Wang, 2002: Impacts of humidity-corrected sonde data on TOGA COARE analyses. *Preprints, 25th Conference on Hurricanes and Tropical Meteorology*, 29 April - 3 May 2002, San Diego, CA.

Del Genio, A. D., M.-S. Yai, W. Kovari, and K. K.-W. Lo, 1996: A prognostic cloud water parameterization for global climate models. *J. Climate*, **9**, 270-304.

Donner, L. J., 1993: A cumulus parameterization including mass fluxes, vertical momentum dynamics, and mesoscale effects. *J. Atmos. Sci.*, **50**, 889-906.

Donner, Leo J., Charles J. Seman, Richard S. Hemler, Songmiao Fan, 2001: A Cumulus Parameterization Including Mass Fluxes, Convective Vertical Velocities, and Mesoscale Effects: Thermodynamic and Hydrological Aspects in a General Circulation Model. *J. Climate*, **14**, 3444-3463.

Duchan, C.E., 1979: Lanczos filtering in one and two dimensions. *J. Appl. Meteor.*, **18**, 1016-1022.

Emanuel, K. A., 1987: An air-sea interaction model of intraseasonal oscillation in the Tropics. *J. Atmos. Sci.*, **44**, 2324-2340.

Fowler, L. D., D. A. Randall, and S. A. Rutledge, 1996: Liquid and ice cloud microphysics in the CSU general circulation model. Part I: Model description and simulated microphysical processes. *J. Climate*, **9**, 489-529.

Frank, W. M., and J. L. McBride, 1989: The vertical distribution of heating in AMEX and GATE cloud clusters. *J. Atmos. Sci.*, **46**, 3464-3478.

Frank, W. M., H. Wang, and J. L. McBride, 1996: Rawinsonde budget analyses during the TOGA COARE IOP. *J. Atmos. Sci.*, **53**, 1761-1780.

Gamache, J. F., and R. A. Houze Jr., 1983: Water budget of a mesoscale convective system in the tropics. *J. Atmos. Sci.*, **40**, 1835-1850.

Gray, M. E. B., 2000: Characteristics of numerically simulated mesoscale convective systems and their application to parameterization. *J. Atmos. Sci.*, **57**, 3953-3970.

Hayashi, Y., and A. Sumi, 1986: The 30-40 day oscillation simulated in an"aqua planet" model. *J. Meteor. Soc. Japan.*, **64**, 451-466.

Hayashi, Y., 1970: A theory of large-scale equatorial waves generated by condensation heat and accelerating the zonal wind. *J. Meteor. Soc. Japan*, **48**, 140-160.

Hayashi, Y., 1971: Large-scale equatorial waves destabilized by convective heating in the presence of surface friction. *J. Meteor. Soc. Japan*, **49**, 458-466.

Hayashi, Y., and D. G. Golder, 1986: Tropical intraseasonal oscillations appering in a GFDL general circulation model and FGGE data. Part I: Phase propagation. *J. Atmos. Sci.*, **43**, 3058-3067.

Hayashi, Y., and D. G. Golder, 1988: Tropical intraseasonal oscillations appearing in a GFDL general circulation model and FGGE data. Part II: Structure. *J. Atmos. Sci.*, **45**, 3017-3033.

Hendon, H. H., and B. Liebmann, 1990: A composite study of onset of the Australia monsoon. *J. Atmos. Sci.*, **47**, 2227-2240.

Hendon, H. H., and M. L. Salby, 1994: The life cycle of the Madden-Julian oscillation. *J. Atmos. Sci.*, **51**, 2225-2237.

Houze, R. A., 1982: Cloud clusters and large-scale vertical motions in the Tropics. *J. Meteor. Soc. Japan*, **60**, 396-410.

Houze, R. A., 1989: Observed structure of mesoscale convective systems and implications for large-scale heating. *Quart. J. Roy. Meteor. Soc.*, **115**, 425-461.

Houze, R. A., 1997: Stratiform precipitation in regions of convection: A meteorological paradox? *Bull. Amer. Meteor. Soc.*, **78**, 2179-2196.

Hu, Q., and D. A. Randall, 1994: Low-frequency oscillations in radiative-convective systems. *J. Atmos. Sci.*, **51**, 1089-1099.

Johnson, R. H., 1984: Partitioning tropical heat and moisture budgets into cumulus and meso-scale components: Implication for cumulus parameterization. *Mon. Wea. Rev.*, **112**, 1590-1601.

Kessler, W. S., and M. J. McPhaden, and K. M. Weickmann, 1995: Forcing of intraseasonal Kelvin waves in the equatorial Pacific. *J. Geophys. Res.*, **100**, 10613-10631.

Krishnamurti, T.-N., P. K. Jayakumar, J. Sheng, N. Surgi, and A. Kuma, 1985: Divergent circulations on the 30 to 50 day timescale. *J. Atmos. Sci.*, **42**, 364-375.

Kummerow, C., J. Simpson, O. Thiele, W. Barnes, A. T. C. Chang, E. Stocker, R. F. Adler, A. Hou, R. Kakar, F. Wentz, P. Ashcroft, T. Kozu, Y. Hong, K. Okamoto, T. Iguchi, H. Kuroiwa, E. Im, Z. Haddad, G. Huffman, B. Ferrier, W. S. Olson, E. Zipser, E. A. Smith, T. T. Wilheit, G. North, T. Krishnamurti, K. Nakamura, 2000: The Status of the Tropical Rainfall Measuring Mission (TRMM) after Two Years in Orbit. *J. of Appl. Meteor.*, **39**, 1965-1982.

Lau, K. M., and P. H. Chan, 1985: Aspects of the 40-50-day oscillation during the northern winter as inferred from outgoing longwave radiation. *Mon. Wea. Rev.*, **113**, 1889-1909.

Lau, K. M., and L. Peng, 1987: Origin of low-frequency (intraseasonal) oscillations in the tropical atmosphere. *J. Atmos. Sci.*, **44**, 950-972.

Lau, K.-M., and T. J. Phillips, 1986: Coherent fluctuations of extratropical geopotential height and tropical convection in intraseasonal timescales. *J. Atmos. Sci.*, **43**, 1164-

1181.

Lau, N. C., I. M. Held, and J. D. Neelin, 1988: The Madden-Julian oscillations in an idealized general circulation model. *J. Atmos. Sci.*, **45**, 3810-3831.

Leary, C. A., and R. A. Houze, 1980: The contribution of mesoscale motions to the mass and heat fluxes of an intense tropical convective system. *J. Atmos. Sci.*, **37**, 2444-2457.

Lee, M.-I., I.-S. Kang, J.-K. Kim, and B.E. Mapes, 2001: Influence of cloud-radiation interaction on simulating tropical intraseasonal oscillation with an atmospheric general circulation model , *J. Geophys. Res.*, **106**, 14219-14233.

Li, J.-L., L. Takacs, and A. Hou, 2002: Validation of moist physical processes in a GCM using TRMM data. TRMM International Science Conference, 22-26 July 2002, Honolulu, Hawaii.

Liebmann, B., H. H. Hendon, and J. D. Glick, 1994: The relationship between t tropical cyclones of the western Pacific and Indian Oceans and the Madden-Julian oscillation. *J. Meteor. Soc. Japan*, **72**, 401-411.

Lin, X., and R. H. Johnson, 1996: Heating, moistening, and rainfall over the western Pacific warm pool during TOGA COARE. *J. Atmos. Sci.*, **53**, 3367-3383.

Lindzen, R. E., 1974: Wave-CISK in the tropics. *J. Atmos. Sci.*, **31**, 156-179.

Madden, R. A., and P. R. Julian, 1971: Detection of a 40-50 day oscillation in the zonal wind in the tropical Pacific. *J. Atmos. Sci.*, **28**, 702-708.

Madden, R. A., and P. R. Julian, 1972: Description of global-scale circulation cells in the tropics with a 40-50 day period. *J. Atmos. Sci.*, **29**, 1109-1123.

Madden, R. A., and P. R. Julian, 1994: Observations of the 40-50-day tropical oscillation-A review. *Mon. Wea. Rev.*, *122*, 814-837.

Mapes, B. E., and R. A. Houze, 1993: Cloud clusters and superclusters over the oceanic warm pool. *Mon. Wea. Rev.*, **121**, 1398-1415.

Mapes, B. E., and R. A. Houze, 1995: Diabatic divergence profiles in western Pacific mesoscale convective systems. *J. Atmos. Sci.*, **52**, 1807-1828.

Molinari, J., and T. Corsetti, 1985: Incorporation of cloud-scale and mesoscale downdrafts into cumulus parameterization: Results of one- and three-dimensional integrations. *Mon. Wea. Rev.*, **113**, 485-501.

Murakami, M., 1979: Large-scale aspects of deep convective activity over the GATE area. *Mon. Wea. Rev.*, **107**, 994-1013.

Murakami, T., and T. Nakazawa, 1985: Tropical 45 day oscillation during the 1979 Northern Hemisphere summer. *J. Atmos. Sci.*, **42**, 1107-1122.

Nakazawa, T., 1986: Intraseasonal variations in the OLR in the Tropics during the FGGE year. *J. Meteor. Soc. Japan*, **64**, 17-34.

Nakazawa, T., 1988: Tropical super clusters within intraseasonal variations over the western Pacific. *J. Meteor. Soc. Japan*, **66**, 823-839.

Neelin, J. D., I. M. Held, and K. H. Cook, 1987: Evaporation-wind feedback and low-frequency variability in the tropical atmosphere. *J. Atmos. Sci.*, **44**, 2341-2348.

Oort, A. H., and J. J. Yienger, 1996: Observed long-term variability in the Hadley circulation and its connection to ENSO. *J. Climate*, **9**, 2751-2767.

Qian, T., and R. D. Cess, 2002: Cloud vertical structure and radiative heating profiles during TOGA COARE. manuscript in preparation.

Randall, D. A., Harshvardhan, D. A. Dazlich, and T. G. Cosetti, 1989: Interactions among radiation, convection, and large-scale dynamics in a general circulation model. *J. Atmos. Sci.*, **46**, 1943-1970.

Raymond, D. J., 2001: A New Model of the Madden-Julian Oscillation. *J. Atmos. Sci.*, **58**, 2807-2819.

Salby, M. L., and H. H. Hendon, 1994: Intraseasonal behavior of clouds, temperature, and motion in the Tropics. *J. Atmos. Sci.*, **51**, 2207-2224.

Salby, M. L., R. B. Garcia, and H. H. Hendon, 1994: Planetary-scale circulations in the presence of climatological and wave-induced heating. *J. Atmos. Sci.*, **51**, 2344-2367.

Sardeshmukh, P. D., 1993: The baroclinic problem and its application to the diagnosis of atmospheric heating rates. *J. Atmos. Sci.*, **50**, 1099-1112.

Sardeshmukh, P. D., M. Newman, and C. R. Winkler, 1999: Dynamically consistent estimates of diabatic heating. *Proceedings, 24th Climate Diagnostics and Prediction Workshop*, Tucson, AZ, 172-175.

Slingo, J. M., and Coauthors, 1996: Intraseasonal oscillations in 15 atmospheric general circulation models: Results from an AMIP diagnostic subproject. *Climate Dyn.*, **12**, 325-357.

Stocker, E., J. Kwiatkowski, O. Kelley, 2001: Gridded Hourly Text Products: A TRMM Data Reduction approach. *Proceedings of IGARSS 2001*, Sydney Australia, 9-13 July 2001.

Sud, Y. C., and G. K. Walker, 1993: A rain evaporation and downdraft parameterization to complement a cumulus updraft scheme and its evaluation using GATE data. *Mon. Wea. Rev.*, **121**, 3019-3039.

Sui, C. H., and K.-M. Lau, 1989: Origin of low-frequency (intraseasonal) oscillations in the tropical atmosphere. Part II. Structure and propagation of mobile wave-CISK modes and their modification by lower boundary forcings. *J. Atmos. Sci.*, **46**, 37-56.

Takayabu, Y .N., T. Iguchi, M. Kachi, A. Shibata, and H. Kanzawa, 1999: Abrupt termination of the 1997-98 El Nino in response to a Madden-Julian oscillation. *Nature*, **402**, 279-282.

Thompson, R. M., S. W. Payne, E. E. Recker, and R. J. Reed, 1979: Structure and properties of synoptic-scale wave disturbances in the Intertropical Convergence Zone of the eastern Atlantic. *J. Atmos. Sci.*, **36**, 53-72.

Tiedtke, M., 1993: Representation of clouds in large-scale models. *Mon. Wea. Rev.*, bf 121, 3040-3061.

Wang, B., and H. Rui, 1990: Dynamics of the coupled moist Kelvin-Rossby wave on an equatorial B-plane. *J. Atmos. Sci.*, **47**, 398-413.

Wang, W., and M. E. Schlesinger, 1999: The dependence on convection parameterization of the tropical intraseasonal oscillation simulated by the 11-layer UIUC atmospheric GCM. *J. Climate*, **12**, 1423-1457.

Weickmann, K. M., G. R. Lussky, and J. E. Kutzbach, 1985: Intraseasonal (30-60 day) flucutations of outgoing longwave radiation and 250 mb streamfunction during northern winter. *Mon. Wea. Rev.*, **113**, 941-961.

Wheeler, M., and G. N. Kiladis, 1999: Convectively coupled equatorial waves: Analysis of clouds and temperature in the wavenumber-frequency domain. *J. Atmos. Sci.*, **56**, 374-399.

Winkler, C. R., M. Newman, and P. D. Sardeshmukh, 2001: A linear model of wintertime low-frequency variability. Part I: Formulation and forecast skill. *J. Climate*, **14**, 4474-4494.

Xie, P., and P. A. Arkin, 1997: Global precipitation: A 17-year monthly analysis based on gauge observations, satellite estimates, and numerical model outputs. *Bull. Amer. Meteor. Soc.*, **78**, 2539-2558.

Yamasaki, M., 1968a: A tropical cyclone model with parameterized partition of released latent heat. *J. Meteor. Soc. Japan*, **46**, 202-214.

Yamasaki, M., 1968b: Detailed analysis of a tropical cyclone simulated with a 13-layer model. *Pap. Meteor. Geophys.*, **19**, 559-585.

Yamasaki, M., 1969: Large-scale disturbances in a conditionally unstable atmosphere in low latitudes. *Pap. Meteor. Geophys.*, **20**, 289-336.

Yanai, M., S. Esbensen, and J.-H. Chu, 1973: Determination of bulk properties of tropical cloud clusters from large-scale heat and moisture budgets. *J. Atmos. Sci.*, **30**, 611-627.

Yanai, M., B. Chen, and W.-W. Tung, 2000: The Madden-Julian oscillation observed during the TOGA COARE IOP: Global view. *J. Atmos. Sci.*, **57**, 2374-2396.

Yasunari, T., 1979: Cloudiness fluctuations associated with the northern hemisphere summer monsoon. *J. Meteor. Soc. Japan*, **57**, 227-242.

Zhang, C., 1996: Atmospheric intraseasonal variability at the surface in the tropical western

Pacific Ocean. *J. Atmos. Sci.*, **53**, 739-758.

Zhang, M. H., and M. A. Geller, 1994: Selective excitation of tropical atmospheric waves in wave-CISK: The effect of vertical wind shear. *J. Atmos. Sci.*, **51**, 353-368.

Zhang, M. H., and J. L. Lin, 1997: Constrained variational analysis of sounding data based on column-integrated budgets of mass, heat, moisture, and momentum: Approach and application to ARM measurements. *J. Atmos. Sci.*, **54**, 1503-1524.

Zhang, M. H., and J. L. Lin, 1999: Synthesizing TOGA COARE measurements in the atmosphere, at the surface, and at TOA. *COARE-98. Proc. Conf. on the TOGA Coupled Ocean-Atmosphere Response Experiment (COARE).* Boulder CO, 7-14 July 1998. WMO/TD 940, 309-310.

FIGURE CAPTIONS

Fig. 1 (a) Standard deviation of the 30-70 day bandpass filtered anomaly of the CMAP precipitation from 1979-1999. The unit is mm/day. The thick solid polygons are the sounding arrays during TOGA COARE. The inner one is the Intensive Flux Array (IFA). The outer one is the Outer Sounding Array (OSA).

(b) The lag-correlation between the 30-70 day CMAP precipitation anomaly and itself at 0N155E.

Fig. 2 The response function of the Murakami filter used in this study.

Fig. 3 The 30-70 day bandpass filtered anomaly of the CMAP precipitation during TOGA COARE (November 1, 1992 to Febuary 28, 1993). The unit is mm/day. The thick dashed line indicates the location of the TOGA COARE sounding arrays.

Fig. 4 The vertical structure of the diabatic heating anomaly in the MJO for (a) TOGA COARE IFA. (b) TOGA COARE OSA. (c) 21 years (1979-1999) of chi-corrected data at 0N155E. The time lag is with respect to the time of maximum precipitation. The heating anomaly has been normalized by its column-integration at the time of maximum precipitation. The unit is (K/day)/(mm/day). The first contour is 0.03, and the contour interval is 0.15. Negative contours are shaded. In (c) only the anomaly with linear correlation above the 95% confidence level is plotted.

Fig. 5 The MJO anomalous vertical heating profile at the time of maximum precipitation for TOGA COARE IFA (thick solid line), TOGA COARE OSA (thick dashed line), and 21 years (1979-1999) of chi-corrected data at 0N155E (thin solid line).

Fig. 6 The precipitation anomaly during the composite life cycle of the MJO for 4 years (1998-2001) of TRMM (a) PR, (b) TMI, and (c) combined data at 0N147E. The thick solid line is the total precipitation. The thin solid line is the convective precipitation. The thin dashed line is the stratiform precipitation.

Fig. 7 Partition of the observed heating profile (thick solid line) into three components: the stratiform component (thin solid line), the radiative component (thin dotted line), and the convective component (thin dashed line).

Fig. 8 (a) Comparison of the observed heating profile with the model heating profiles. The thick solid line is the observed heating profile. All other lines are the model heating profiles. The models include the GFDL GCM used in Lau et al. 1988 (thick dashed line), the University of Illinois GCM used in Wang and Schlesinger (1999)'s A3 experiment (thin solid line) and M2 experiment (thin dotted line), the Seoul National University GCM used in Lee et al. 2001 (thin dashed line), and the theoretical model of Sui and Lau (1989)'s deep convection case (thin dot-dashed line). (b) The difference between the observed heating profile and the model heating profiles.

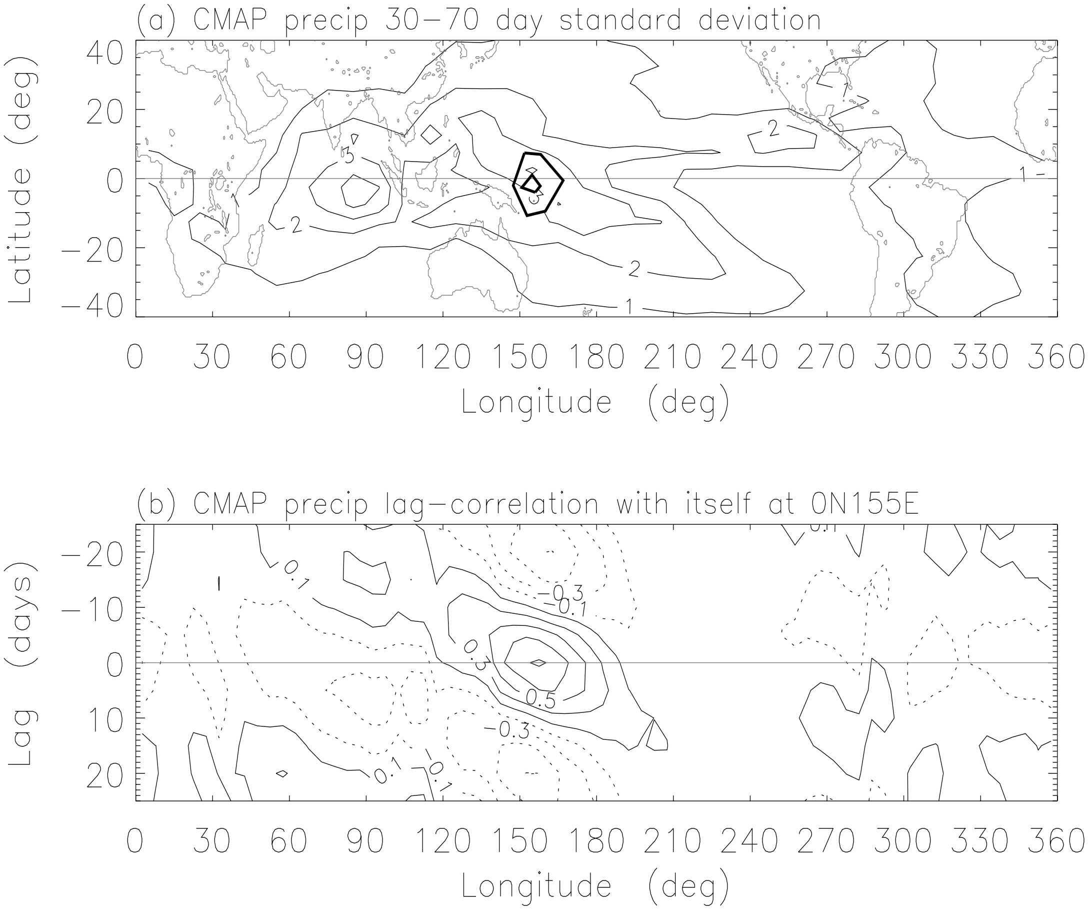

(a) CMAP precip 30−70 day standard deviation
Latitude (deg)
Longitude (deg)
(b) CMAP precip lag−correlation with itself at 0N155E
Lag (days)
Longitude (deg)

Figure 1:

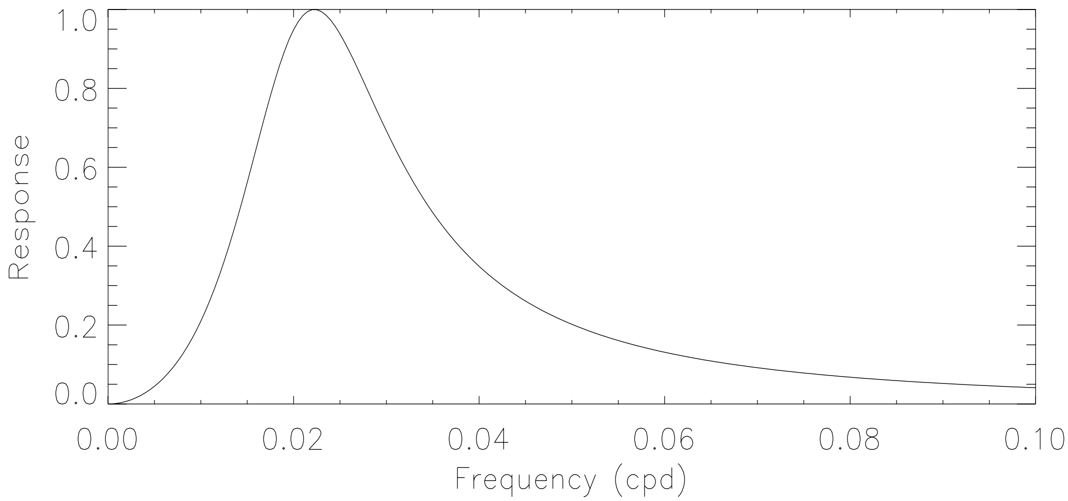
1.0
0.8
0.6
0.4
0.2
0.0
Response
0.00
0.02
0.04
0.06
0.08
0.10
Frequency (cpd)

Figure 2:

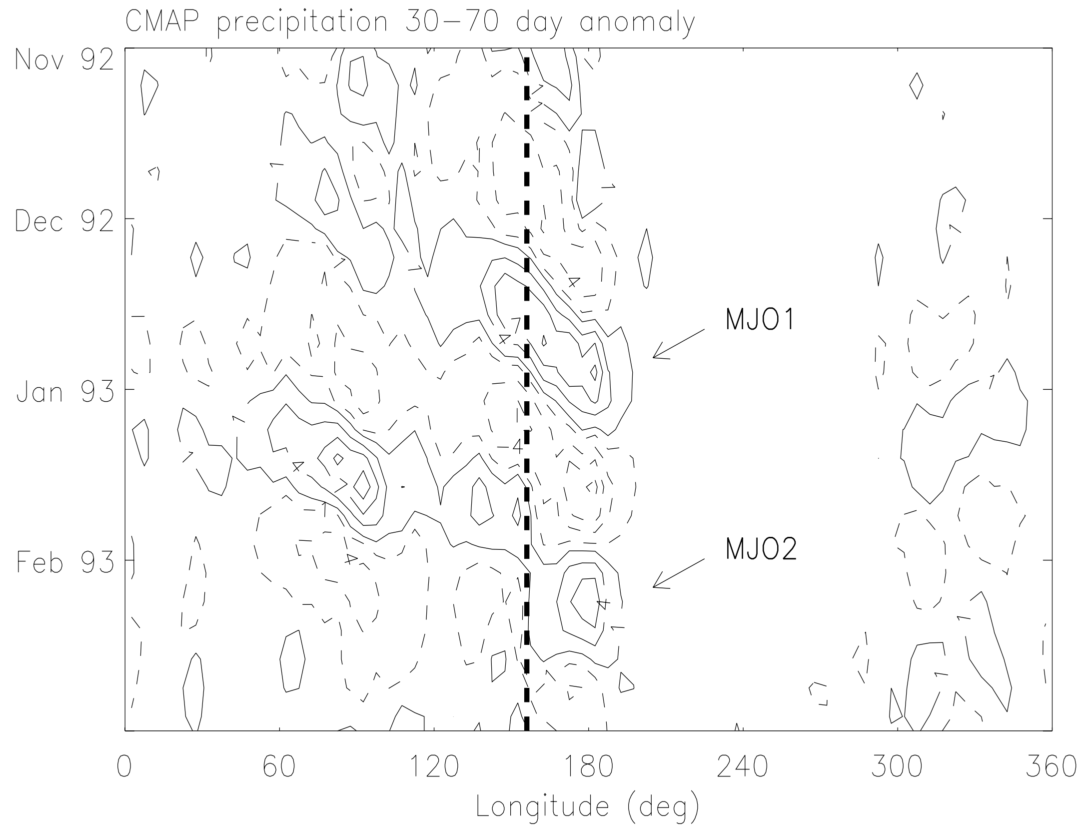
CMAP precipitation 30-70 day anomaly
Nov 92
Dec 92
Jan 93
Feb 93
MJO1
MJO2
0
60
120
180
240
300
360
Longitude (deg)

Figure 3:

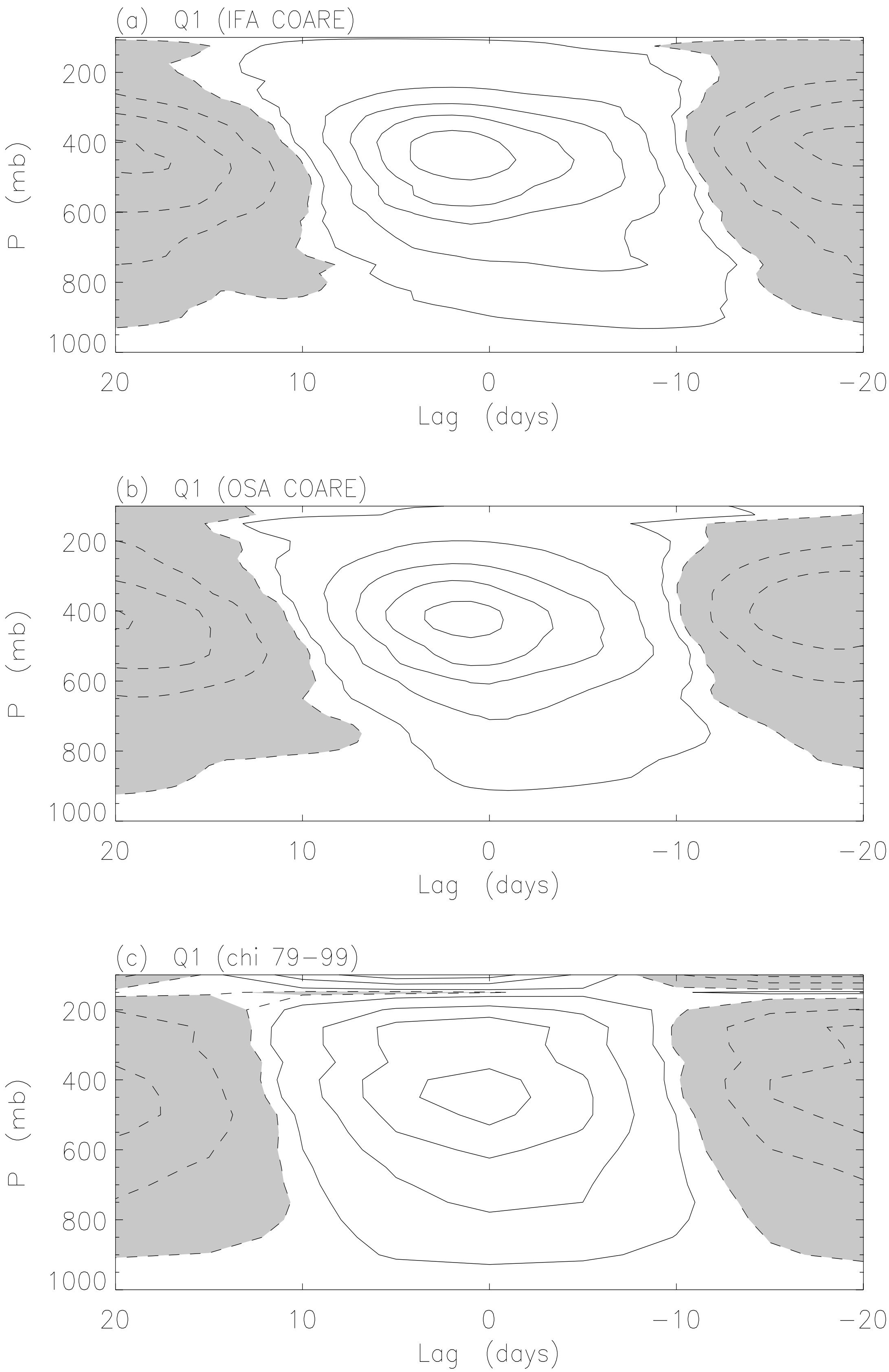
(a) Q1 (IFA COARE)
(b) Q1 (OSA COARE)
(c) Q1 (chi 79-99)
P (mb)
200
400
600
800
1000
20
10
0
−10
−20
Lag (days)

Figure 4:

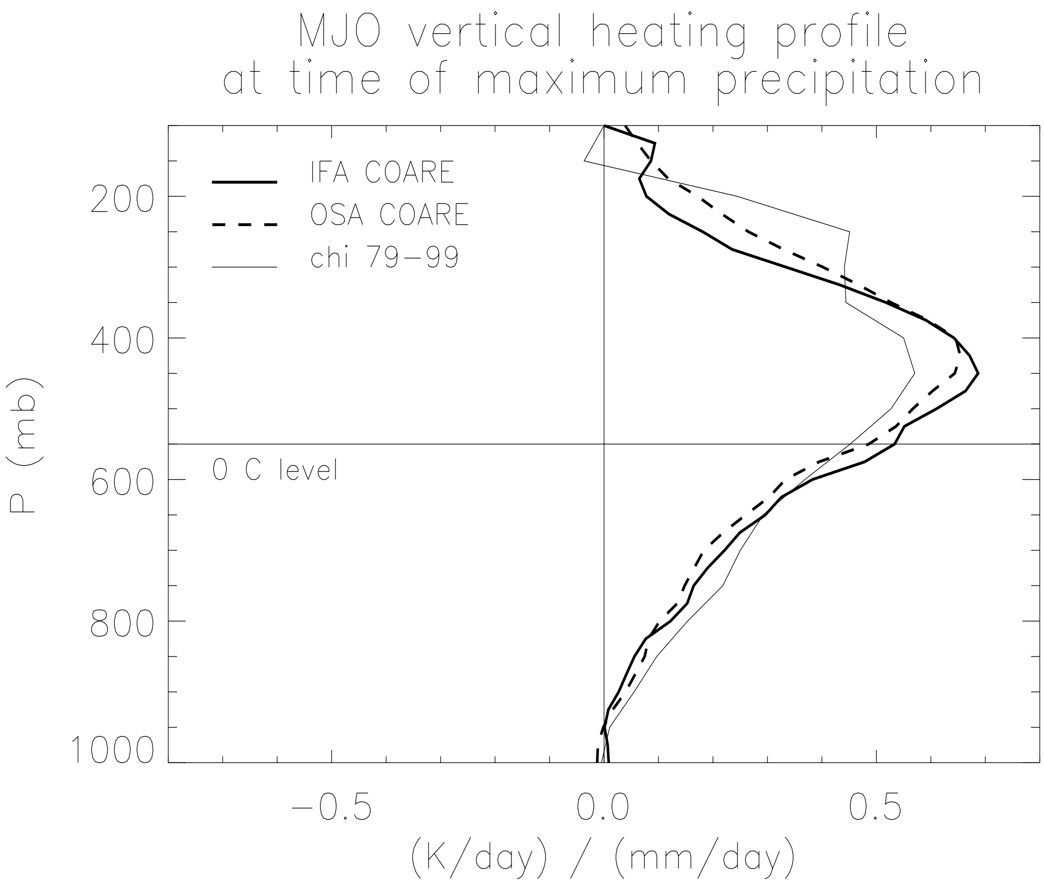
MJO vertical heating profile
at time of maximum precipitation
IFA COARE
OSA COARE
chi 79-99
0 C level
200
400
600
800
1000
P (mb)
−0.5
0.0
0.5
(K/day) / (mm/day)

Figure 5:

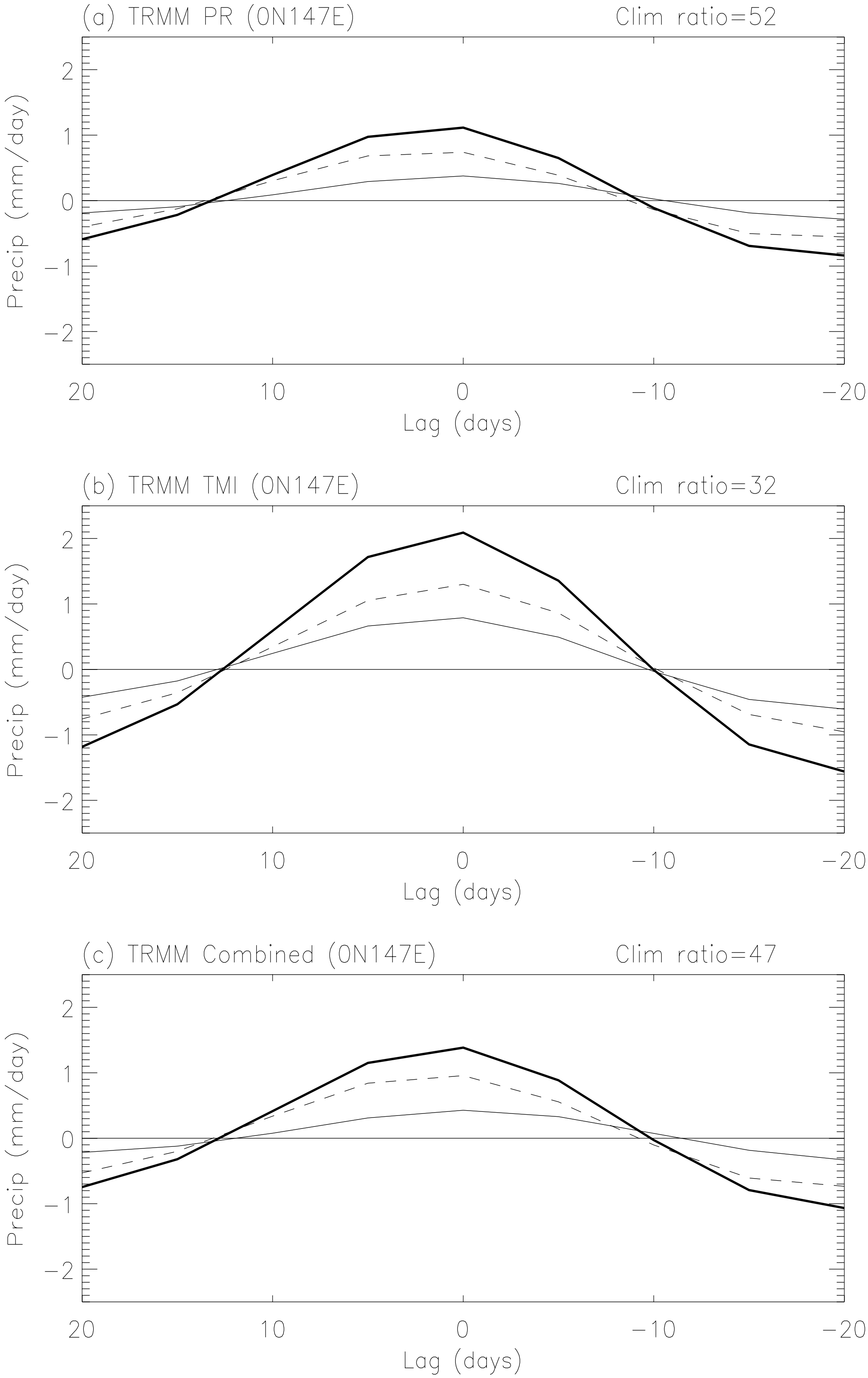

(a) TRMM PR (0N147E)
Clim ratio=52
Precip (mm/day)
Lag (days)
(b) TRMM TMI (0N147E)
Clim ratio=32
Precip (mm/day)
Lag (days)
(c) TRMM Combined (0N147E)
Clim ratio=47
Precip (mm/day)
Lag (days)

Figure 6:

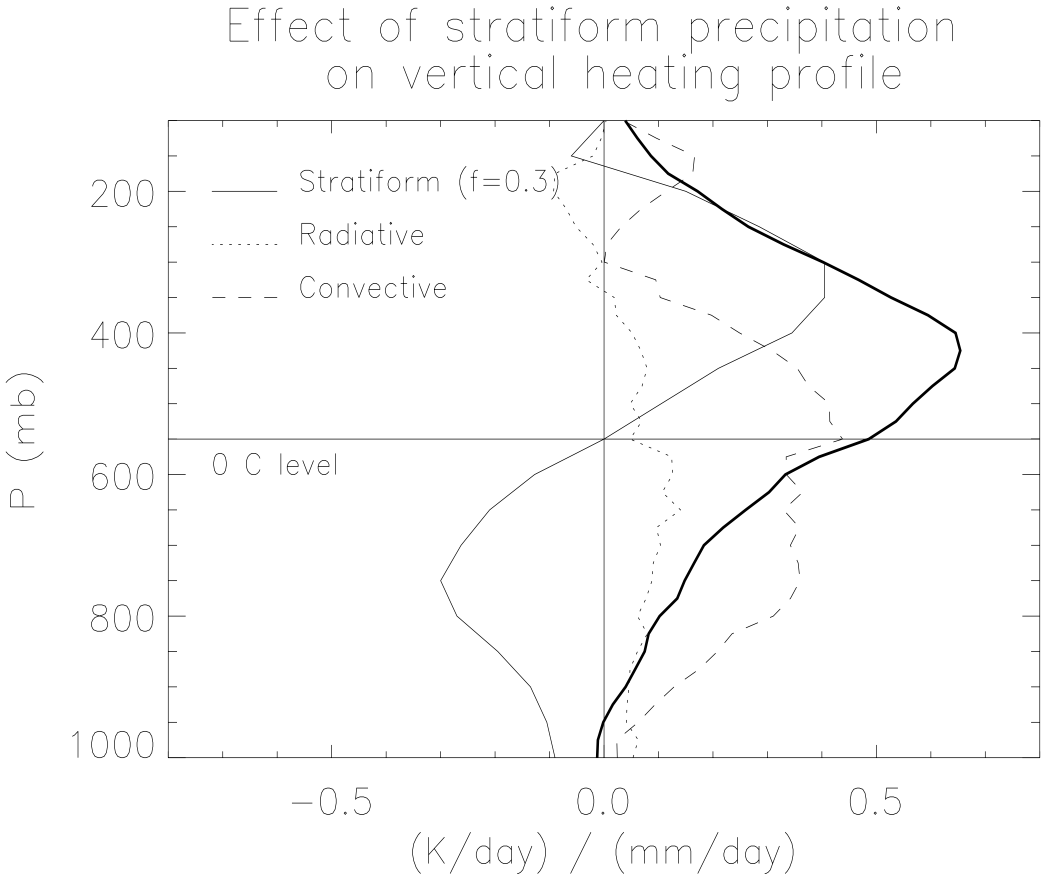

Effect of stratiform precipitation
on vertical heating profile
Stratiform (f=0.3)
Radiative
Convective
0 C level
P (mb)
200
400
600
800
1000
−0.5
0.0
0.5
(K/day) / (mm/day)

Figure 7:

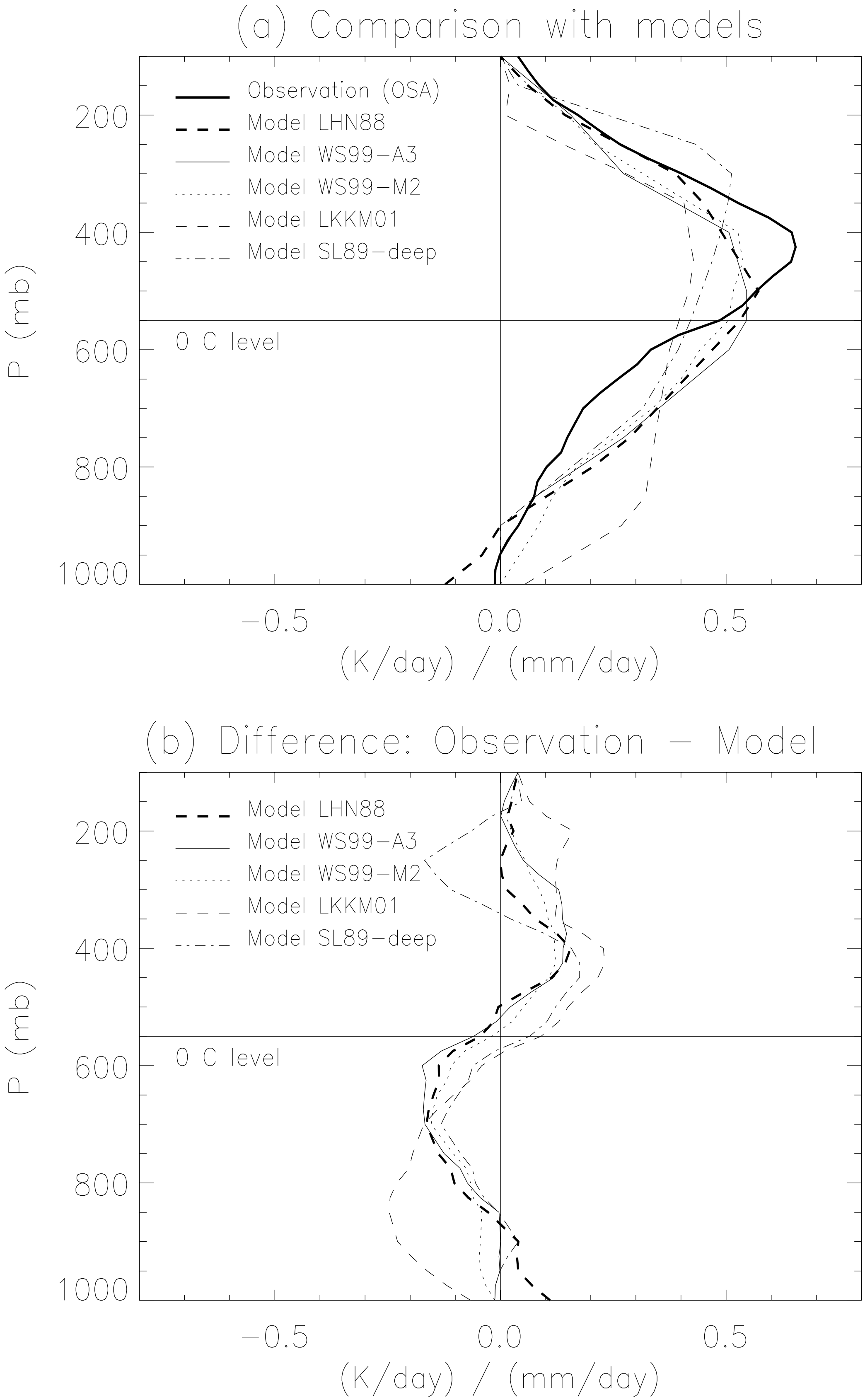

(a) Comparison with models
Observation (OSA)
Model LHN88
Model WS99-A3
Model WS99-M2
Model LKKM01
Model SL89-deep
0 C level
P (mb)
200
400
600
800
1000
-0.5
0.0
0.5
(K/day) / (mm/day)
(b) Difference: Observation - Model
Model LHN88
Model WS99-A3
Model WS99-M2
Model LKKM01
Model SL89-deep
0 C level
P (mb)
200
400
600
800
1000
-0.5
0.0
0.5
(K/day) / (mm/day)

Figure 8: